# CHAPTER II

# RELEVANT THEORY AND LITERATURE REVIEWS

## 2.1 Relevant theory

### 2.1.1 Biomaterials

#### 2.1.1.1 Silk [7-10]

*1. The nature of silk*

Silk is naturally occurring protein produced by *Lepidoptera larvae* species including silkworms, spiders, scorpions, mites, butterflies and moths, which form their cocoons. Cocoon especially from silkworms, have been used commercially as biomedical sutures for decades and used in textile production for centuries. Silk is a fibrous protein synthesized in specialized epithelial cells that line glands in these organisms, followed by secretion into the lumen of these glands where the protein is stored prior to spinning into fibers. The most widely studied silks are cocoon silk from *Bombyx mori* silkworms and dragline silk from *Nephila clavipes* spiders, due to their impressive mechanical properties which are the advantage for textile and biomedical applications.

Silk in its natural form is composed of a filament core protein, silk fibroin, and a glue-like coating consisting of a family of sericin proteins, as shown in Figure 2.1.

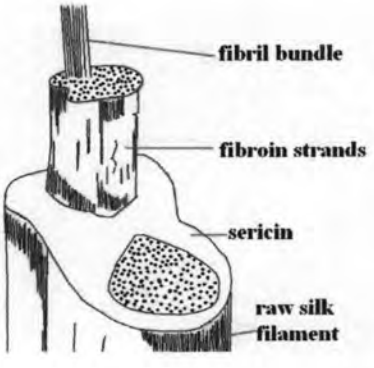


**Figure 2.1** Structure of raw silk fiber [11].

Sericin is the water-soluble glue-like protein that binds the fibroin fibers together. It is brittle, and inelastic. The amount of sericin ranges from 20-25wt% of raw silk fiber depending on the type of cocoon. Sericin is a macromolecular protein which has the molecular weight ranges vary from 10 to over 300 kDa. Removal of the sericin from silk fibroin is accomplished by a process called "degumming" using acid or soap.

A major constituent of raw silk fiber, about 75-80wt%, is silk fibroin. It is an insoluble fibrous protein that is biocompatible with living tissues. Its structure is composed of layers of antiparallel beta pleated sheets (Figure 2.2) which run parallel to the silk fiber axis. Silk fibroin fibers are about 10-25 μm in diameter and composed of heavy (~350 kDa) and light (~25 kDa) polypeptide fractions connected by disulfide linkages. The disulfide linkage between the Cys-c20 ($20^{th}$ residue from the carboxyl terminus) of the heavy chain and Cys-172 of the light chain holds the fibroin together and a P25 (a 25 kDa glycoprotein) is noncovalently linked to these proteins. The heavy chains consist of 12 repetitive regions interspersed with 11 non repetitive regions. The repetitive regions are responsible for the formation of crystalline β-sheet structures which the non-repetitive regions are amorphous.

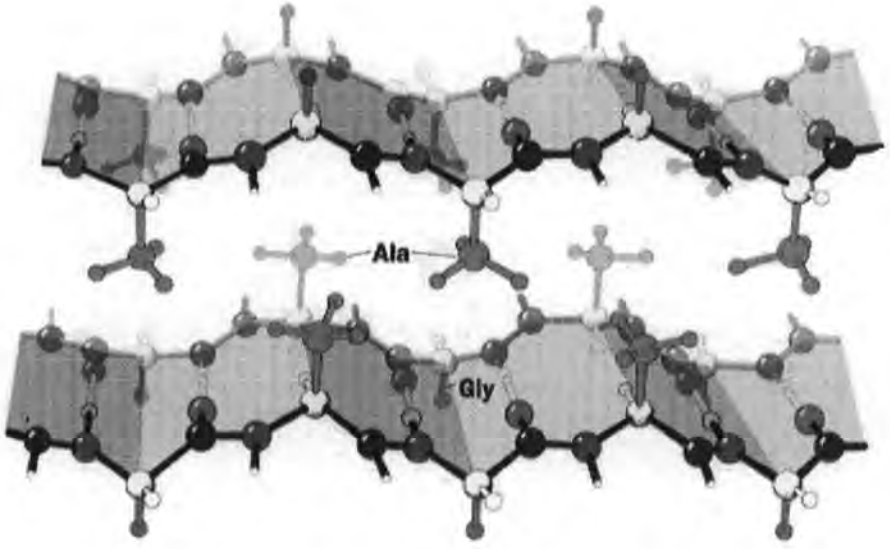


**Figure 2.2** Structure of silk fibroin [12].

*2. Amino acid compositions and molecular structure of Bombyx mori silk fibroin*

*Bombyx mori* silk fibroin consists of 18 amino acids (Table 2.1) and most of which have strongly polar side groups such as hydroxyl, carboxyl, and amino groups. The isoelectric point is around 3.

**Table 2.1** Amino acid compositions (%) of silk fibroins extracted from different *Bombyx mori* cocoons [13].

| Amino acid | Silk fibroins | | | |
|---|---|---|---|---|
| | Yellow | White | Pink | Green |
| **Glycine, Gly*** | 50.0 | 48.8 | 51.0 | 47.0 |
| **Alanine, Ala*** | 24.7 | 27.0 | 24.5 | 25.4 |
| **Serine, Ser*** | 10.8 | 9.8 | 9.6 | 10.9 |
| **Tyrosine, Tyr*** | 4.7 | 5.0 | 4.8 | 1.4 |
| **Valine, Val*** | 2.7 | 2.7 | 2.9 | 2.8 |
| **Threonine, Thr°** | 0.9 | 1.0 | 1.0 | 0.9 |
| **Isoleucine, Ile+** | 2.0 | 1.2 | 1.6 | 1.7 |
| **Phenylalanine, Phe+** | 0.7 | 0.7 | 0.8 | 0.9 |
| **Lysine, Lys°** | 0.8 | 1.1 | 0.9 | 1.2 |
| **Aspartic Acid, Asp °** | 0.5 | 0.7 | 0.6 | 1.4 |
| **Leucine, Leu+** | 0.5 | 0.6 | 0.6 | 0.7 |
| **Arginine, Arg°** | 0.4 | 0.5 | 0.5 | 0.4 |
| **Glutamic Acid, Glu°** | 0.7 | 0.5 | 0.6 | 1.4 |
| **Proline, Pro+** | 0.5 | 0.5 | 0.5 | 0.4 |
| **Methionine, Met+** | Nd | Nd | Nd | Nd |
| **Histidine, His°** | Nd | Nd | Nd | Nd |
| **Cysteine, Cys** | Nd | Nd | Nd | Nd |
| **Trytophan, Trp** | Nd | Nd | Nd | Nd |

*Amino acid forming the repetitive exapeptides (H-chain): Gly, Ala, Ser, Tyr, Val

+Non-polar amino acid: Ile, Leu, Phe, Met, Pro

°Basic amino acid: Asp, Glu, Arg, Thr, Lys, His

Nd: not detected.

The primary structure of *Bombyx mori* silk fibroin was generally divided into four regions as shown in Figure 2.3. Region 1 is the highly repetitive Gly-Ala-Gly-Ala-Gly-Ser sequence which constitutes the crystalline part of the fibroin (94% of total chain). Region 2 is the relatively less repetitive Gly-Ala-Gly-Ala-Gly-Tyr and/or Gly-Ala-Gly-Ala-Gly-Val-Gly-Tyr sequences consisting of the semi-crystalline parts. Region 3 is Gly-Ala-Gly-Ala-Gly-Ser-Gly-Ala-Ala-Ser and Region 4 is the amorphous part containing charged and aromatic residues.

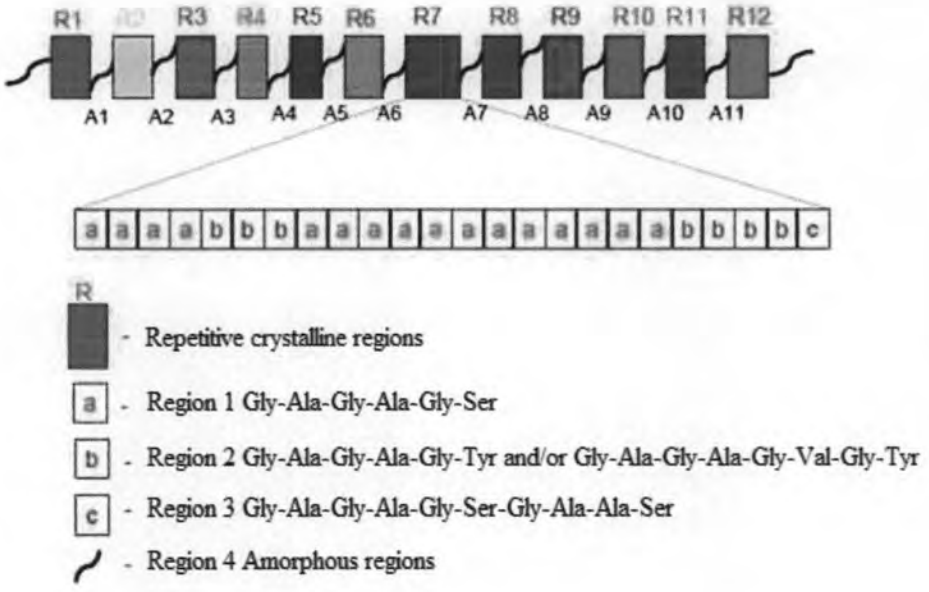


**Figure 2.3** Schematic representation of the primary structure of *Bombyx mori* silk fibroin [14].

*3. <u>Thai silk</u>* [15]

Thai silk is one of *Bombyx mori* silkworms which mainly produced for the textile industry in the northern and north-eastern parts of Thailand. Characteristics of Thai silk are yellow color and coarse filaments. It also contains more silk gum (up to 38%) than other types of *Bombyx mori* silk (20-25%). There are around 28 species of Thai silk such as Nangnoi Srisaket 1, Nangline and other species of blended-Thai silk such as blended-Sakolnakorn and blended-Ubonratchathani 60-35 (lotus).

- Nangnoi Srisaket 1

This specy is easily cultivated. The life cycle is short, approximately 18 days and the color of the cocoon is dark yellow.

- Nangline

This specy is easily degummed. The color of cocoon is dark yellow. The weight of cocoon is 0.68 – 1.64 g and the length of silk fiber is about 311 m/cocoon.

- Blended-Ubonratchathani 60-35

This specy is the blend between Ubonratchathani 60 and Nangnoi Srisaket 1. The color of cocoon is yellow. The weight of cocoon is 1.4 g and the length of silk fiber is about 519 m/cocoon.

*4. Applications of silk*

It is well known that silk thread has been used clinically as sutures. In addition, it is used in many applications including textile industry, cosmetics and medical applications. Attractive properties of silk fibroin include its robust mechanical properties when hydrated, biocompatibility, biodegradability, high dissolved-oxygen and water-vapor permeability, and resistance against enzymatic degradation. Examples of products made from silk in medical applications are, wound covering materials, gauze pads and bandaged, silk clothes for protecting affected parts (incised wound, burn, tumor, bedsore, etc.), artificial skin, cell-growth substrates, oxygen-permeable membranes, and tissue-engineered scaffolds, as shown in Figure 2.4.


**Figure 2.4** Applications of silk [16].

### 2.1.1.2 Gelatin [17-19]

*1. The nature of gelatin*

Gelatin is a natural protein polymer, which is the product obtained by breaking the triple-helix structure of collagen into single-stranded macromolecules through thermal denaturation or a combination of physical and chemical degradation. Gelatin is a vitreous, translucent and brittle solid that is faintly yellow to light tan, nearly tasteless and odorless. Generally, gelatin is supplied in various physical forms such as coarse granules, fine powders and leaves.

An important property of gelatin in aqueous solution is a thermally reversible conformational transition, which is responsible for inducing gelation upon cooling from solution below the specific gel point of gelatin as the chains undergo a conformational coil-to-helix transition during which they tend to recover the collagen triple-helix structure. At ambient temperature, gelatin molecules form networks wherein the triple-helixes serve as physical cross-link sites. Upon heating to body temperature (37°C), the triple-helixes dissolve due to denaturation, and gelatin again becomes fully soluble. The gel point is dependent on the source of the raw material. Gelatin extracted from the tissues of warm-blooded animals has a gel point in the range of 30°C to 35°C and gelatin extracting from the skin of cold-water ocean fish has a gel point in the range of 5°C to 10°C. When immersing in cold water, gelatin granules were hydrated into discrete, swollen particles. On being warmed, gelatin disperses into the water, resulting in a stable suspension. Gelatin is stable in aqueous solutions of polyhydric alcohols such as glycerine and propylene glycol. It is insoluble in most organic solvents [20].

*2. Type of gelatin*

There are two types of gelatin, depending on the preparation process as shown in Figure 2.5.

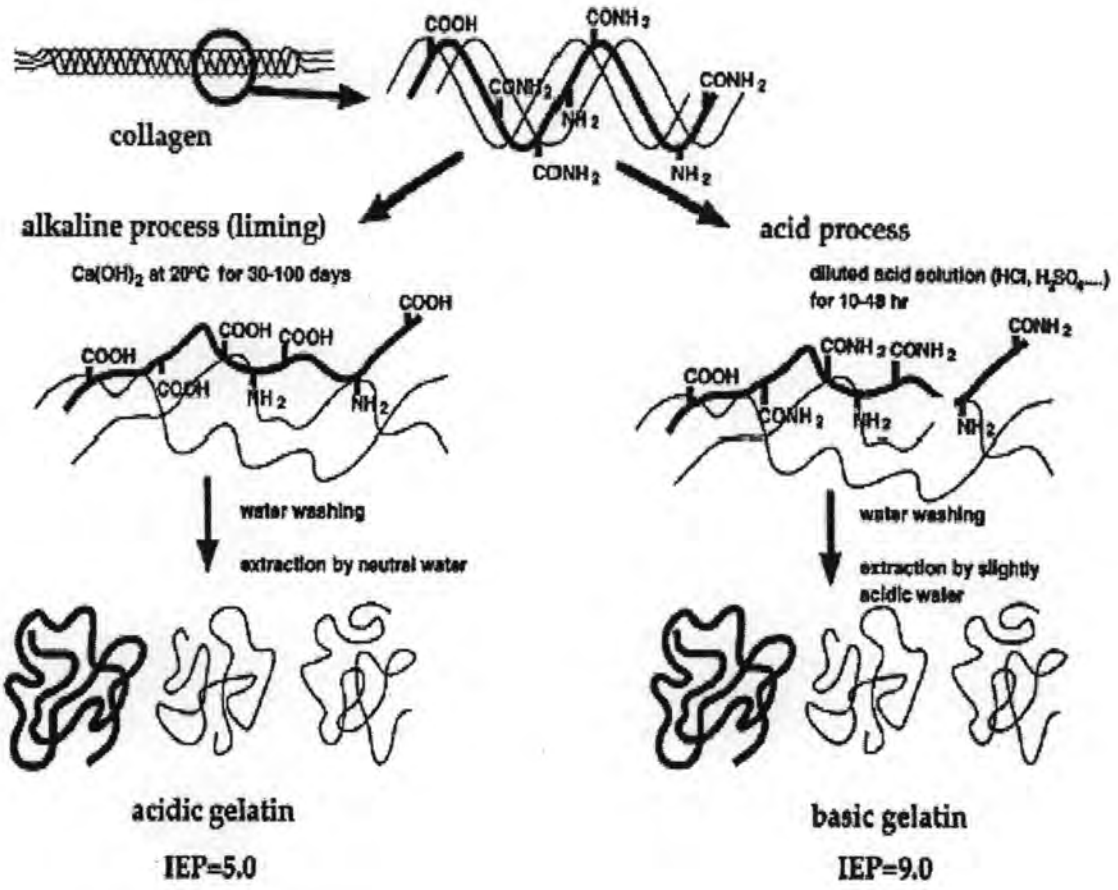


**Figure 2.5** Preparation process for acidic and basic gelatins from collagen [21].

1. Basic gelatin (Type A gelatin) is produced by an acidic pretreatment before thermal denaturation of collagenous raw materials. This method is especially suitable for less crosslinked materials such as pig skin collagen (pig skin collagen is less complex than the bovine collagen). Acid process is faster than alkaline process and normally requires 10 to 48 hours of denaturation. Type A gelatin exhibits an isoelectric point between 7 to 9.

2. Acidic gelatin (Type B gelatin) is produced by lime processing or an alkaline pretreatment before thermal denaturation of collagenous raw materials. This method is suitable for more complex collagen as found in bovine hides, cattle hides

and bones. The purpose of the alkaline pretreatment is to destroy certain chemical crosslinkages presenting in collagen molecule by converting amide residues of asparagine and glutamine into aspartic and glutamic acid. This leads to a 25% higher carboxylic acid content and higher viscosity of type B gelatin than type A gelatin. This process requires longer time, normally several weeks. Type B gelatin exhibits an isoelectric point between 4.7 to 5.4. Typical specifications for type A and B gelatin are shown in Table 2.2.

**Table 2.2** Typical specifications for gelatins [22].

| Property | Type A | Type B |
|---|---|---|
| **pH** | 3.8-5.5 | 5.0-7.5 |
| **Isoelectric Point** | 7.0-9.0 | 4.7-5.4 |
| **Gel strength (bloom)** | 50-300 | 50-300 |
| **Viscosity (mps)** | 15-75 | 20-75 |
| **Ash (%)** | 0.3-2.0 | 0.5-2.0 |

*3. Structural unit and composition*

Gelatin has random coil structure which can be readily soluble in water. Its contains many glycine (almost 1 in 3 residues, arranged every third residue), proline and 4-hydroxyproline residues. A typical structure is -Ala-Gly-Pro-Arg-Gly-Glu-4Hyp-Gly-Pro- as shown in Figure 2.6.

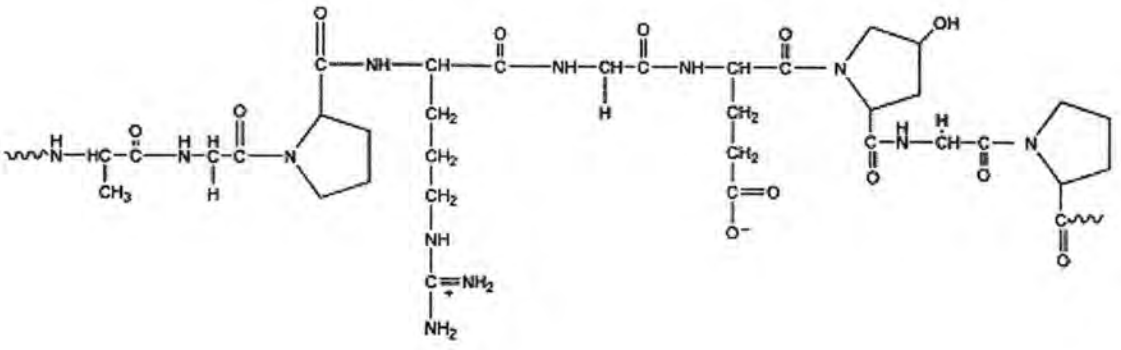

**Figure 2.6** The structural unit of gelatin [19].

Generally, gelatin contains 84-90% protein, 1-2% mineral salts and 8-15% water. Its contains specific amounts of 18 different amino acids as shown in Table 2.3.

**Table 2.3** Amino acid compositions of gelatin [23].

| **Amino acid** | **Wt%** |
|---|---|
| Arginine | 7.8 |
| Glutamic acid | 10.0 |
| Histidine | 0.8 |
| Hydroxyproline | 11.9 |
| Leucine | 3.3 |
| Methionine | 0.7 |
| Proline | 12.4 |
| Theronine | 2.1 |
| Valine | 2.2 |
| Alanine | 8.9 |
| Asperic acid | 6.0 |
| Glycine | 21.4 |
| Hydroxylysine | 1.0 |
| Isoleucine | 1.5 |
| Lycine | 3.5 |
| Phenylanine | 2.4 |
| Serine | 3.6 |
| Tyrosine | 0.5 |
| **Total** | **100** |

*4. Applications of gelatin*

Gelatin is biocompatible, biodegradable and nonimmunogenic, therefore it is suitable for biomedical applications, such as vascular prosthetic sealants, wound dressing formulation, tissue-engineered scaffolds, and drug delivery system, e.g., as hard and soft capsules, hydrogel, or microspheres. In addition, it has been commonly used as pharmaceutical, photography and cosmetic manufacturing. It is also used extensively in foods as a gelling agent, stabilizer, thickener and clarification of juices. Common examples of foods that contain gelatin are gelatin desserts, jelly, trifles,

aspic, marshmallows, ice cream, jams, yogurt and margarine etc. Examples of gelatin applications are shown in Figure 2.7.

**Figure 2.7** Applications of gelatin [11].

### 2.1.1.3 Hydroxyapatite [24-27]

*1. The nature of hydroxyapatite*

Hydroxyapatite, also called hydroxylapatite (HA), is a naturally occurring mineral. It has a occurring form of calcium apatite with the formula of $Ca_5(PO_4)_3(OH)$, but is usually written as $Ca_{10}(PO_4)_6(OH)_2$ to denote that the crystal unit cell comprises two molecules. Some commercially available hydroxylapatite particles have a size range between 10-40 μm with a Ca/P ratio of 1.62, while other sources had a size range of 160-200 μm with a Ca/P ratio of 1.66 to 1.69. Its crystallized structure has a hexagonal form. The structure of hydroxyapatite is shown in Figure 2.8. Hydroxyapatite is also the main mineral component of bones and hard tissues in mammals; 70% of bone is made up of the inorganic mineral hydroxyapatite

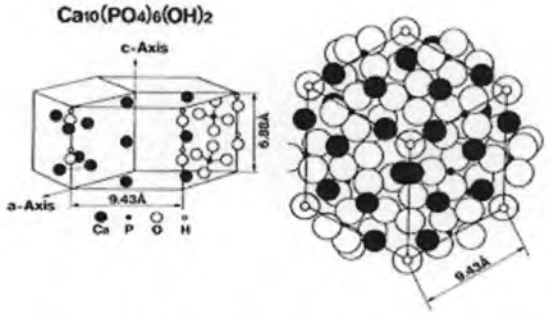


**Figure 2.8** Structure of hydroxyapatite [28].

*2. Properties of hydroxyapatite*

Naturally occurring appatite has brown, yellow or green color while the pure hydroxyapatite is white. Hydroxyapatite has a specific gravity of 3.08 and its Mohs hardness scale is 5. Is a thermally unstable compound and decomposed at temperature about 800 - 1200°C depending on its stoichiometry. Hydroxyapatie integrated in bone structures is bioactive and supports bone ingrowth, without breaking down or resorbing.

*3. Applications of hydroxyapatite*

Hydroxyapatite is a compound of great interest in catalysis, in the industry of fertilizers, protein chromatography, bioceramic coatings and water treatment procedures. It is also used in the preparation of bioactive materials because it is the inorganic crystalline constituent in vertebrates calcified hard tissues such as bone and teeth. Hydroxyapatite may be employed in forms of powders, porous blocks or beads to fill bone defects or voids when large sections of bone are removed (e.g. bone cancers) or when bone augmentations are required (e.g maxillofacial reconstructions or dental applications). The bone filler acts as a scaffold and encourage the rapid filling of the void by naturally forming bone. Treatment using bone filler can reduce healing times compared to the case of empty defect.

### 2.1.2 Tissue-engineered scaffolds [29-30]

There are some basic requirements that have been widely accepted for designing tissue-engineered scaffolds.

1. The scaffold should be biocompatibility and positively interact with cells, including enhanced cell adhesion, growth, migration, and differentiated function.
2. The scaffold should possess interconnecting pores of appropriate scale to favour tissue integration and vascularisation, and have high porosity, surface area and proper pore size.
3. The scaffold should be made from biodegradable or bioresorbable material in which the natural regenearating tissue can eventually replace. A proper degradation rate is also needed to match the rate of neotissue formation.

4. The scaffold must have the appropriate mechanical integrity to maintain the tissue structure.
5. The scaffold should be easily fabricated into a variety of shapes and sizes.

### 2.1.3 Scaffold fabrication techniques [29-32]

In the body, tissues are organized into three-dimensional structures. To engineer functional tissues and organs successfully, the scaffolds must be designed to support the formation of new tissue in three dimensions, to promote cell migration and adhesion as well as to foster the transport of nutrients and metabolic wastes.

Several techniques have been developed to produce the porous three-dimensional scaffolds, including freeze drying, porogen leaching, gas foaming, fiber meshes/fiber bonding, phase separation and melt molding. It this research, the first three tecniques were introduced for scaffolds fabrication.

#### 2.1.3.1 Freeze drying technique [31]

The scaffolds in this research were fabricated using a freeze drying (lyophilization) process in which freeze drying is process water or other solvent is removed from the frozen sample by a sublimation process. Sublimation occurs when a frozen liquid goes directly to gas phase without passing through the intermediate formation of liquid phase. During by sublimation is different from evaporation at ambient temperatures which usually results in changes of the product. The basis for this sublimation process involves the absorption of heat by the frozen sample in order to vaporize the ice; the use of a vacuum pump to enhance the removal of water vapor from the surface of the sample; the transfer of water vapor to a collector; and the removal of heat by the collector in order to condense the water vapor. In essence, the freeze drying process is a balance between the heat absorbed by the sample to vaporize the ice and the heat removed from the collector to convert the water vapor into ice.

*1. Freezing and lyophilizing rates*

The efficiency of the freeze drying process is dependent upon these factors including the surface area and the thickness of the sample, the collector temperature and vacuum obtained the eutectic point and solute concentration of the sample.

The thickness of the sample should be only a few milliliters. However, for larger volumes, the samples should be shell frozen to maximize the surface area and minimize the thickness of the sample. The volume of the freeze dry flask should be 2-3 times of the sample.

To dry the sample, solvent must be removed from the frozen sample via sublimation. This is accomplished by the collector and the vacuum pump. The collector, which should be at least 10 to 15°C colder than the eutectic temperature (melting temperature) of the sample, traps vapor as ice. Since the vapor pressure at the collector is lower than that of the samples, the flow of water vapor is from the sample to the collector. Because the vapor diffusion process occurs very slowly under normal atmospheric conditions, a good vacuum is essential to maintain an efficient rate. In most applications, the maintenance of a vacuum at 133 x $10^{-3}$ mBar or less is required for freeze drying.

*2. Freeze drying of volatile solvent*

In same cases, the samples to be freeze dried contain volatile solvents such as acetic acid, formic acid or pyridine. These solvents can have an effect on the eutectic temperature and increase the vapor pressure at the surface of the sample. Also, compared to water, samples that contain volatile solvents require less heat absorption for sublimation to occur. Hence, the samples become easier to melt. Using a diluted solvent for freeze drying can help to keep the sample frozen. For example, a 0.2 M acetic acid solution is much easier to freeze dry than a 0.5 M solution.

### 2.1.3.2 Porogen-leaching technique

Porous scaffolds can also be prepared using porogen-leaching technique. Porogen is a desired-shape insoluble particle that used to form pores of scaffold. A polymer solution is usually cast into the porogen-filled mold. After the evaporation of the solvent, the porogens are leached out with water to create interconnected pores in structure of the scaffold. The pore size and porosity of scaffold can be controlled by

the size of the porogen particles and the porogen/polymer ratio, respectively. Examples of the porogens used for this technique include sodium chloride, glucose, camphor, monosodium- glutamate, and alginate hydrogel.

#### 2.1.3.3 Gas foaming technique

Gas can also be used as porogens. Process of gas foaming involves the production of gases from the physical or chemical methods to produce pores of the scaffolds. This method can be used to produce homogeneous pore system with pore size ranging from 100 nm-1 μm. Surfactant or stabilizer is required to stabilize the bubbles in solution.

### 2.1.4 Crosslinking techniques [33-38]

Crosslinking can be used to prolong degradation rate and improve biomechanical characteristics (typically to match those characteristics of the target tissue), however, but it might affect biocompatibility of materials. Protein crosslinking can be acchived by various methods such as ultraviolet irradiation, electron beam irradiation, dehydrothermal treatment, enzyme (i.e. transglutaminase), and chemical treatment.

#### 2.1.4.1 Chemical crosslinking

Choice of crosslinking agent is based on the reactive group(s) presented in materials. For example, materials which have amine groups usually use glutaraldehyde (GA) for the crosslinking. The disadvantage of chemical crosslinking is the cytotoxicity of some crosslinking agents, including glutaraldehyde, formaldehyde, and epoxy compounds when left in the scaffolds. As a result, 1-ethyl-3-(3-dimethylaminopropyl)carbodiimide, hydrochloride (EDC) has became of interest. EDC is a zero-length crosslinking agent in which the agent itself is not incorporated into the macromolecule. Moreover, it has not been shown to cause any cytotoxic reactions. EDC is also heterobifunctional agent, which contains 2 different reactive groups that are able to directly crosslink 2 different amino acid side groups. This agent is generally utilized as a carboxyl activating agent for amide bonding with

primary amines. The chemical structure of EDC is shown in Figure 2.9. Therefore, it was suitable for crosslinking of silk fibroin and gelatin in this research.

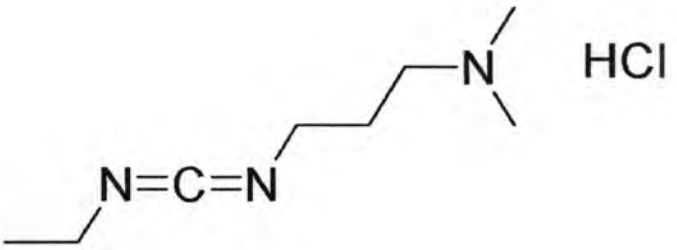


**Figure 2.9** Chemical structure of EDC [33].

EDC is water soluble, up to 100 mg/ml, so the crosslinking can be achieved in physiologic solutions without adding organic solvent. EDC reacts with the carboxylic functional groups of aspartic and glutamic amino acids on molecule #1, forming an amine-reactive *O*-acylisourea intermediate. This intermediate may react with the amine functional groups of lysine and hydroxylysine amino acids on adjacent proteins (molecule #2). The crosslink, anisopeptide bond or amide bond (that mimics the natural peptide bonds in proteins), is formed, and bridged neighboring polypeptide chains. However, the intermediate is also susceptible to hydrolysis, making it unstable and short-lived in aqueous solution. The addition of *N*-hydroxysuccinimide (NHS) or *N*-hydroxysulfosuccinimide (Sulfo-NHS) stabilizes the amine-reactive *O*-acylisourea intermediate by converting it to an amine-reactive NHS-ester intermediate which is much more stable in solution, thus increasing the efficiency of EDC-mediated coupling reactions. The amine-reactive NHS-ester intermediate has sufficient stability to permit two-step crosslinking procedures, which allows the carboxyl groups on one protein to remain unaltered. The EDC crosslinking mechanism is showed in Figure 2.10. Excess EDC and crosslinking byproducts (e.g., a urea derivative) can be easily removed by washing with water or dilute acid.

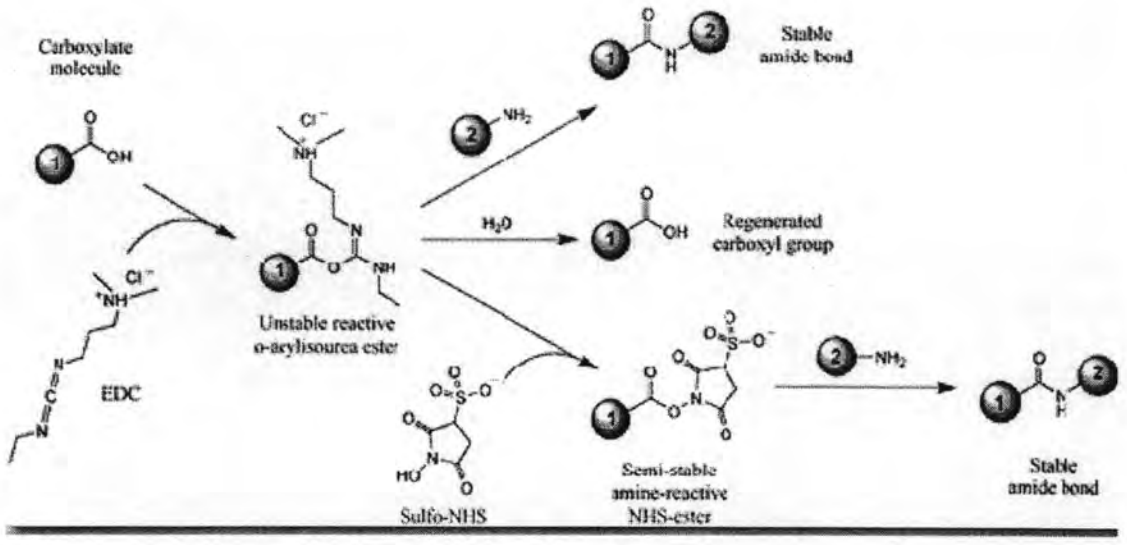


**Figure 2.10** Crosslinking of protein with EDC and NHS [35].

### 2.1.4.2 Ultraviolet irradiation

UV irradiation generates radicals at the aromatic residues of amino acids. The binding of these radicals will react to each other, resulting in crosslinking formation. The crosslinking density largely changes depending on UV irradiation time. When the irradiation time is short, UV irradiation will enable protein to crosslink intermolecularly. However, it is possible that irradiation for longer time preferably acts on the chain scission of protein molecules. A balance of the crosslinking and chain scission will result in unchanged density of crosslinking.

### 2.1.4.3 Electron beam irradiation

Electron beam irradiation also produces radicals. The number of crosslinks is not large and the water content does not decrease very much. This is because the chain scission by the over dose of electron beam also occurs.

### 2.1.4.4 Dehydrothermal treatment (DHT)

Dehydrothermal treatment operates in a vacuum oven, at temperature above 100°C. DHT generates chemical bonding between the amino and carboxyl groups of proteins molecules due to thermal dehydration. DHT is based on the condensation

reactions between adjacent amino acid side chains. It seems that the number of cross-linking sites is few because the cross-linking sites are restricted to adjacent functional groups in the condensation reaction.

### 2.1.5 Nature of cells

Types of cell culture are classified into two types as follow:

#### 2.1.5.1 Primary cell cultures [1, 39]

Primary cell cultures are obtained directly from multiple mammalians including mouse, guinea pig, rat, rabbit, dog, horse, and human. These cells can be kept at the differentiated state for a short period, days to weeks. Functionally differentiated primary cell cultures have a limited life span, and although maintenance of the differentiated properties has been improved by additives to the culture medium, components of the extracellular matrix or by different forms of co-culture, cell specific functions will eventually decline.

Mesenchymal stem cells, one type of primary cells, can be isolated from a wide variety of tissues including; adult tissues such as fat, hair follicles and scalp subcutaneous tissue, periodontal ligament, thymus and spleen, as well as pre-natal tissues, such as placenta, umbilical cord blood, fetal bone marrow, periosteum, synovium, muscle, adipose tissue, blood, lung, liver, and spleen. In this work, mesenchymal stem cells isolated from marrow are called bone marrow-derived stem cells (MSCs), as shown in Figure 2.11.

MSCs can be expanded and differentiated into cells of different connective tissue lineages including bone, cartilage, fat, and muscle upon proper stimulation. These cells also have the potential for a wide range of therapeutic applications through autologous, allogeneic or xenogeneic stem cell transplantation. MSCs have been used to treat a variety of defects and diseases, including critical size segmental bone defects, full thickness cartilage defects, tendon defects, myocardial infarction and even nerve defects.

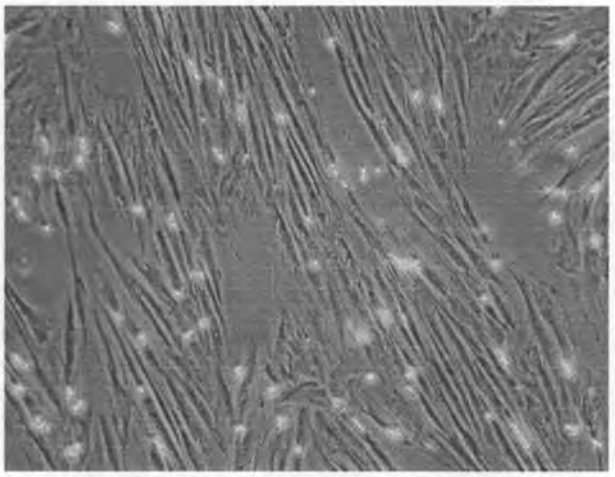

**Figure 2.11** Bone marrow-derived stem cells (MSCs) [40].

### 2.1.5.2 Permanent cultures or cell lines cultures [1, 41]

Cell lines cultures have an unlimited proliferation capacity. They are derived from embryos, tumors or transformed cells. Examples of cell lines are L929 mouse skin fibroblast, MC3T3-E1 mouse osteoblast, HeLa, MDCK, etc. Cell lines can proliferate and/or differentiate, both with different limitations, depending on the cell type studied. Numerous publications provide protocols for the isolation of different cell types, their culture conditions, and for the evaluation of the degree of differentiation.

MC3T3-E1, preosteoblastic cell line, was derived from mouse calvaria. Culture conditions can be induced to undergo a developmental sequence leading to the formation of multilayered bone nodules. This sequence is characterized by the replication of preosteoblasts followed by growth arrest and expression of mature osteoblastic characteristics such as matrix maturation and eventual formation of multilayered nodules with a mineralized extracellular matrix. This cell line has become the standard *in vitro* model of osteogenesis and has found widespread use in studies examining many aspects and applications of osteogenesis, including transcriptional regulation, mineralization and tissue engineering.

L929 (Figure 2.12) is a fibroblast-like cell line cloned from strain L. The parent strain was derived from normal subartaneous areolar and adipose tissue of a male C3H/An mouse.

**Figure 2.12** L929 mouse skin fibroblast [41].

## 2.2 Literature reviews

The literature reviews are summarized into three parts as follows:

1. Preparation and characterization of crosslinked gelatin and silk fibroin.
2. Preparation and characterization of gelatin/silk fibroin and collagen/silk fibroin systems.
3. Preparation and characterization of hydroxyapatite/silk fibroin, hydroxyapatite/gelatin and hydroxyapatite/collagen biomaterials.

### 2.2.1. Preparation and characterization of crosslinked gelatin and silk fibroin

**Tomihata, K. *et.al.* [4]**

In 1996, Tomihata *et.al.* compared crosslinking of gelatin films by the use of two types of carbodiimide. A water-soluble carbodiimide; 1-ethyl-3-(3-dimethylaminopropyl)carbodiimide, hydrochloride (EDC) was more effective for gelatin crosslinking than a water-insoluble carbodiimide; 1,3-dicyclohexyl carbodiimide (DCC). Mechanism of gelatin crosslinking performed in a simple reaction of a solid form under a heterogeneous condition. It was also found that the

optimal ethanol concentration in the ethanol-water mixtures, which were used as the reaction medium to prevent dissolution of gelatin films, was around 80vol%. The lowest water content of the crosslinked gelatin film attained by water swelling was 55wt%, and the optimal reaction temperature and time for crosslinking with water-soluble carbodiimide ranged between 15-25°C and 24 h, respectively. It was concluded that gelatin crosslinked with carbodiimides was as effective as that crosslinked with glutaraldehyde but showed non-toxicity.

**Kundu, J. *et.al.* [42]**

In 2008, Kundu *et.al.* characterized the biophysical, rheological, thermal, mechanical, and biological properties of the silk gland fibroin films, compared with cocoon fibroin from the *Bombyx mori* mulberry silkworms. Fibroin solutions showed increased turbidity, non-Newtonian and shear thinning behavior at higher concentration. The films after methanol treatment were mechanically stronger, moderately swelled and less hydrophilic. The spectroscopy studies of the silk gland fibroin films showed the presence of amide I, amide II and amide III peaks and the conformational transition from random coil to β-sheet on methanol treated silk films. The Raman spectroscopy results of silk gland fibroin films showed strong peaks in regions 1157, 1523, 1007 $cm^{-1}$ which were absent in the silk cocoon fibroin films. X-ray diffraction (XRD) studies of the films showed peaks at $2\theta=22.37^{o}$ (silk I conformation), 14.16 and $28.44^{o}$ (both peaks denoting the silk II conformation) on the methanol-treated silk gland fibroin films, similarly to the untreated films. The XRD diffraction profiles between both silks were different. Atomic force microscopy (AFM) studies showed that surfaces of the methanol-treated silk gland fibroin films were rougher than the untreated films. The matrices were biocompatible and supported L929 mouse fibroblast cell growth and proliferation. The results substantiated the silk gland fibroin films as potential biomaterial matrices.

### 2.2.2 Preparation and characterization of gelatin/silk fibroin and collagen/silk fibroin systems

**Meinel, L. *et.al.* [43]**

In 2004, Meinel *et.al.* have cultured human bone marrow-derived mesenchymal stem cells (hMSCs) on porous scaffolds made from silk (slow degrading), silk-RGD (slow degrading, enhanced cell attachment), and collagen (fast degrading) in control and osteogenic medium. Histological analysis and microcomputer tomography (micro-CT) showed the development of up to 1.2-mm-long interconnected and organized bone-like trabeculae with cuboid cells on the silk-RGD scaffolds. This feature still presented but with a lesser extent on silk scaffolds and absent on the collagen scaffolds. Biochemical analysis showed increased mineralization on silk-RGD scaffolds compared with either silk or collagen scaffolds after 4 weeks. Expression of bone sialoprotein, osteopontin, and bone morphogenetic protein-2 was significantly higher for hMSCs cultured in osteogenic medium than those cultured in control medium both after 2 and 4 weeks of the culture. The results suggested that silk-RGD scaffolds were particularly suitable for autologous bone tissue engineering because of their stable macroporous structure, tailorable mechanical properties matching those of native bone, and slow degradation.

**Gil, E.S. *et.al.* [20]**

In 2005, Gil *et.al.* examined the swelling and protein release kinetics of gelatin/silk fibroin (G/SF) hydrogels varying in composition at temperatures below and above the helix $\rightarrow$ coil (h $\rightarrow$ c) transition of gelatin. G/SF hydrogels were prepared by blending gelatin with amorphous *Bombyx mori* silk fibroin and promoting β-crystallization of silk fibroin via subsequent exposure to aqueous methanol solutions. The swelling behavior of these hydrogels reveals that β-crystallization was virtually complete only after 5 min of exposure to 75/25 w/w methanol/water solution and sensitive to methanol concentration in the aqueous methanol solutions. The results demonstrated that, gelatin and gelatin-rich mixed hydrogels displayed moderate swelling with negligible mass loss in aqueous solution at 20°C, resulting in porous polymer matrixes upon solvent removal. When the solution temperature was

increased beyond the h→c transition of gelatin to body temperature (37°C), these gels exhibit much higher swelling with considerable mass loss, indicating that the dissolved triple-helix conformation of gelatin permitted greater water sorption and protein as gelatin molecules were slowly released into the surrounding aqueous solution.

**Gil, E.S. *et.al.* [5]**

In 2005, Gil *et.al.* investigated the effect of β-sheet crystals on the thermal and rheological behavior of gelatin/silk fibroin (G/SF) hydrogels. G/SF hydrogels with various compositions were prepared by blending type A gelatin with amorphous *Bombyx mori* silk fibroin and subsequently induced the crystallization of silk fibroin upon exposure to 75/25 w/w methanol/water solution for 2 h at 20°C. Thermal calorimetry and dynamic rheology results showed that the silk fibroin chains which possessed a random coil conformation within the G/SF gels had a little effect on the helix→coil (h→c) transition of gelatin. Silk fibroin could dilute the stabilizing efficacy of the triple-helix crosslink sites, and reduce the dynamic elastic modulus of G/SF gels. On the other hand, if the silk fibroin chains possessed a β-sheet conformation, they could shift the h→c transition of gelatin to higher temperature at sufficiently high concentration. This increased the dynamic elastic modulus of the G/SF gels and also stabilized the hydrogels at higher temperatures, comparing to the untreated gels. Even in the presence of silk fibroin β-crystalline network, the h→c transition of gelatin is found to be thermally reversible between ambient and body temperature.

**Gil, E.S. *et.al.* [8]**

In 2006, Gil *et.al.* studied the effects of solvent-induced crystallization and composition in gelatin/silk fibroin (G/SF) hydrogels. After exposure to aqueous methanol solutions, silk fibroin underwent a conformational change from random coil to β-sheet. According to infrared spectroscopy (FTIR) and wide-angle x-ray diffraction (WAXD), this transformation occurred in pure silk fibroin as well as in each of the G/SF blends rapidly, typically within a few minutes. Thermal calorimetry

(DSC) revealed the existence of relatively low temperature thermal transitions (*T*g and *T*c) in untreated silk fibroin and G/SF blends. These transitions disappeared entirely upon MeOH treatment. Thermal gravimetric analysis (TGA) indicated that the formation of the β-sheet structure generally improved thermal stability at elevated temperatures, enhanced the mechanical properties such as tensile modulus, elongation, and tensile strength of the blends, and stabilized gelatin-based hydrogels.

**Lv, Q. *et.al.* [6]**

In 2007, Lv *et.al.* prepared silk fibroin/collagen hydrogels by crosslinking silk fibroin/collagen solutions with different contents of 1-ethyl-3-(3-dimethylaminopropyl)carbodiimide, hydrochloride (EDC). The hydrogels were formed via freeze-drying method. The weight percentage of silk fibroin and collagen in dried blend scaffolds was fixed as 80% and 20%, respectively. It was found that, when the weight percentage of EDC was above 10%, especially 20% and 30%, compared with silk fibroin/collagen dried scaffolds without EDC, the stiff silk fibroin/collagen hydrogels were formed (storage modulus >10 kPa by rheological analysis). Furthermore, these hydrogels can maintain their configuration above 80°C and still maintain the mobility of silk fibroin molecules. The growth of vascular smooth muscle cells (VSMCs) in silk fibroin/collagen gels indicates that the crosslinking reaction has no negative influence on the biocompatibility of these gels. Therefore the stiff silk fibroin/collagen hydrogel has better cytocompatibility than silk fibroin/collagen scaffold, an excellent biomaterial for tissue engineering.

### 2.2.3 Preparation and characterization of hydroxyapatite/silk fibroin, hydroxyapatite/gelatin and hydroxyapatite/collagen biomaterials

**Chang, M.C. *et.al.* [44]**

In 2003, Chang *et.al.* developed biomimetic process, for the formation of organized hydroxyapatite (HA) – gelatin (G) nanocomposites. The HA nanocrystals were precipitated in aqueous solution of G at pH 8 and 38°C. The coprecipitated HA–G nanocomposites showed chemical bonding between calcium ions of HA and carboxyl ions of G molecules which induced a red shift of the 1339 $cm^{-1}$ band of G in

FT-IR analysis. A self-organized of HA nanocrystals along G fibrils was observed in TEM images and electron diffraction patterns. The concentration ratio of G to HA greatly influenced the nucleation and the development of HA nanocrystals. A higher concentration of G induced the formation of tiny crystallites (4 nm×9 nm size), while a lower concentration of G contributed to the development of bigger crystallites (30 nm×70 nm size). From TGA-DTA data, the HA-G nanocomposites showed typically three exothermic temperatures consisting of the thermal degradation and pyrolyzation of G molecules, and the final thermal degradation of the residual organics. The increase in decomposition temperatures indicated the formation of a primary chemical bond between HA and G.

**Wang, L. *et.al.* [45]**

In 2005, Wang *et.al.* prepared hydroxyapatite (HA)-based nanocomposite solid via a wet-mechanochemical route with either untreated and alkali pretreated silk fibroin powders (USF and ASF). Silk fibroin powders were treated using an alkali solution (NaOH 0.05 M) attempting to disentangle their surface fibrils and to enhance the effective contact between the mineral and the organic particles. With the ASF involved, Vickers microhardness of the composite increased by 57%. A more enhanced three-dimensional porous network with a homogenous particle form and a uniform pore size distribution were observed through the intimate crosslinkage between HA clusters and silk fibroin fibrils. In addition, ASF increased the viscosity and the rigidity of the composite solid, and promoted its gelation process, which is favorable for healing bone defects by an injection technique.

**Takahashi, Y. *et.al.* [46]**

In 2005, Takahashi *et.al.* fabricated gelatin sponges incorporating $\beta$TCP by chemical crosslinking of gelatin with glutaralydehyde in the presence of $\beta$TCP at different amounts (0, 25, 50, 75, and 90wt%). All sponge had an interconnected porous structure with the pore size range of 180–200 μm and the porosity around 96%. The compressive modulus of sponges increased with an increase in the amount of $\beta$TCP incorporated. When seeded into the sponges by an agitated method ($5\times10^6$

cells/sponge), MSC were homogeneously distributed throughout the sponge. The morphology of cells attached were more spreaded on the sponges incorporating higher $\beta$TCP amount. The rate of MSC proliferation depended on the $\beta$TCP amount and culture method: the higher proliferation rate was achieved in the case of higher $\beta$TCP amount in the stirring culture. The deformed extent of sponges was suppressed with the increased amount of $\beta$TCP. When measured to evaluate the osteogenic differentiation of MSC, the ALP activity and osteocalcin content became maximum for the sponge with a $\beta$TCP amount of 50wt%. On the contrary, for the static culture, no effect of the $\beta$TCP amount on the ALP activity was observed. Although both the values were significantly high in the stirring culture compared with those in the static culture. These results will give fundamental information to design the scaffolds suitable for bone tissue engineering.

**Tanaka, T. *et.al.* [47]**

In 2007, Tanaka *et.al.* evaluated the efficiency of a nano-scaled hydroxyapatite/silk fibroin (nano-HA/SF) sheet as bone-regeneration scaffolds using rat bone marrow mesenchymal cells (MMCs). The nano-HA/SF sheets were prepared by mixing of methacryloxypropyl trimethoxysilane, ammonium peroxodisulfate, pentaethylene glycol dodecyl ether and silk fibroin fibers in tube. The polymerization was conducted at 50°C for 50 min and then washed with ethanol and dried in a vacuum for 1 h at 60°C. Poly(MPTS)-grafted SF was soaked in the solution of nano-HA particles for 1 h at room temperature. Then it was heated at 120°C for 2 h in a vacuum. The experiments demonstrated that the nano-HA/SF sheets showed good initial cell attachment and supported cell proliferation. After 14 days of culturing, under osteogenic conditions, the alkaline phosphatase (ALP) activity and bone-specific osteocalcin secretion of the cells on nano-HA/SF sheets were higher than silk fibroin sheets. The nano-HA particles supported good cell adhesion to the nano-HA/SF sheets because the roughness of sheet surface was increased. Furthermore, cell adhesion molecules such as fibronectin in serum or the molecules produced by the cells could more easily support cellular adhesion and proliferation since many proteins weree actively adsorbed on HA surfaces. These results indicated that the HA support the osteogenic diffentiation of MMCs. Therefore, the nano-

HA/SF sheet is an effective biomaterial and is applicable in bone reconstruction surgery.

**Kino, R. *et.al.* [48]**

In 2007, Kino *et.al.* used silk fibroin (SF) and hydroxyapatite (HA)-deposited silk fibroin film to prepare multilayered films by alternating lamination. HA-deposited SF films were prepared from SF solution containing 5wt% $CaCl_2$ by air drying, treated with methanol vapor and then soaked in simulated body fluid. The multilayered HA/SF films had HA layers with approximate thickness of 3 – 5 μm and SF layers with thickness of 40 –70 μm. The multilayered HA/SF films were prepared by alternating lamination at 130°C for 4 min to achieve a higher bonding strength and a higher β-sheet content. The comparison of mechanical strength between the multilayered HA/SF films and multilayered SF films indicated that HA layers increased mechanical strength of the films. The biocompatibility and osteoconductivity of HA-deposited SF films were analyzed by culturing of mice osteoblasts (MC3T3-E1). The results indicated that HA-deposited SF films and SF films show similar degrees of cell adhesion and alkaline phosphatase activities.

**Du, C. *et.al.* [49]**

In 2008, Du *et.al.* fabricated *bombyx mori* silk fibroin (SF) and hydroxyapatite (HA) composite films, using glycerin as an additive, by the method of co-precipitation. The theoretical HA content was varied from 2w/w% to 31w/w%. The results showed that the SF/HA composite films were smooth and transparent with the uniform distribution of HA at a low level of HA content (the HA content was lower than 21w/w%). XRD and TGA data showed that the SF in the composites was predominantly in a β-sheet crystalline structure, which was induced not only by the addition of glycerin but also by the HA crystal growth during the composite fabrication, leading to the thermal stable composite films. On the other hand, the HA crystals had the anisotropic growth with high extent of lattice imperfection and the preferential orientation along c-axis, probably promoted by the SF. The results on mechanical testing showed that both break strain and stress were

declined with the increase of HA content in the composites, presumably due to the original brittleness of HA compound.

**Venugopal, J. *et.al.* [50]**

In 2008, Venugopal *et.al.* fabricated electrospun nanofibrous scaffolds, type I collagen (Col) was dissolved in 1,1,1,3,3,3-hexafluoro propanol (HFP) under stirring conditions overnight. Ratio of Col/HA at 1:1 was used and dissolved in HFP and stirred for 2 days. Electrospun nanofibers of collagen and Col/HA were showed interconnected porous structure and the fiber diameters were in the range of 265 ± 0.64 and 293 ± 1.45 nm respectively. The crystalline HA (29 ± 7.5 nm) loaded into the collagen nanofibers were embedded within nanofibrous matrix of the scaffolds. Osteoblasts grew favorably on both nanofibrous scaffolds and showed insignificant level of proliferation. Mineralization was significantly ($p<0.001$) increased to 56% in Col/HA nanofibrous scaffolds compared to collagen. The Alizarin Red-S (ARS) staining also proved increased mineralization after 10 days of osteoblast culture on Col/HA nanofibrous scaffolds. Energy dispersive X-ray analysis (EDX) spectroscopy results indicated that the cells were able to attach and grow on Col/HA nanofibrous scaffolds to form mineralized tissue, which primarily consists of calcium and phosphorous deposits. Therefore, the designed electrospun Col/HA composite nanofibrous scaffold was a potential biomaterial for bone tissue engineering.

**Pek, Y.S. *et.al.* [51]**

In 2008, Pek *et.al.* created a porous collagen-apatite nanocomposite foams as bone regeneration scaffolds that resembled natural bone both chemically and structurally. The nanocomposite scaffolds were prepared by mixing 32.5wt% of collagen fibers extracted from rat skin (T1C) with 67.5wt% of synthetic apatite nanocrystals (carbonated apatite (CAP)-hydroxyapatite (HAP) mixture), where CAP:HAP weight ratio; 0:5, 1:4, 2:3, 3:2, 4:1, and 5:0. These nanocomposite samples were further crosslinked by EDC/NHS. This treatment involved the immersion of samples in a carbodiimide solution containing 14 mM of EDC and 5.5 mM of NHS at room temperature for 2 h. The PA-FTIR spectra and XRD patterns of nanocomposite scaffolds revealed that CAP:HAP at weight ratio of 4:1 showed the most match in

chemical and crystalline structure with trabecular bone. Therefore CAP:HAP at weight ratio of 4:1 was used in all further case. By optimizing the composition and processing parameters, a foam-like nanocomposite material was attained with similar porous microstructure, pore size distributions and mechanical properties (compressive stiffness = $37.3 \pm 2.2$ MPa and yield strength = $2.7 \pm 0.1$ MPa) to those of the trabecular bone. This material also exhibited excellent biocompatibility and bioactivity for promoting MC3T3 cells attachment and proliferation. In addition formation of new bone structures and scaffold mineralization were observed when the scaffolds were implanted at ectopic sites. It was also successfully healed critical-sized defects in the femur of Wistar rats and the tibia of Yorkshire–Landrace pigs. These *in vivo* studies suggested that the nanocomposite scaffolds were biocompatible and osteoinductive.